Pergamon

Geochimica et Cosmochimica Acta, Vol. 60, No. 4, pp. 679–692, 1996

0016-7037/96 $15.00 + .00

0016-7037(95)00429-7

Cosmogenic chlorine-36 from calcium spallation

J. O. STONE,[1] G. L. ALLAN,[2,*] L. K. FIFIELD,[2] and R. G. CRESSWELL[2]

[1]Research School of Earth Sciences, The Australian National University, Canberra, ACT 0200, Australia
[2]Department of Nuclear Physics, Research School of Physical Sciences and Engineering, The Australian National University, Canberra, ACT 0200, Australia

(*Received March* 22, 1995; *accepted in revised form November* 21, 1995)

Abstract—Calcium is a major target element for cosmogenic ^{36}Cl production. Consequently ^{36}Cl rapidly reaches detectable levels in minerals such as calcite and calcium feldspar exposed at the Earth's surface. Spallation of calcium isotopes typically accounts for 80–90% of ^{36}Cl production in these minerals, with subsidiary contributions from negative muon capture by ^{40}Ca and thermal neutron capture by ^{35}Cl. To provide a basis for surface exposure dating, we have calibrated cosmogenic ^{36}Cl production in calcium feldspar from the 17,300 year old Tabernacle Hill basalt. At an altitude of 1445 m and an effective geomagnetic latitude of 40.9° the calcium spallation rate is 152 ± 11 atoms (g Ca)$^{-1}$ a^{-1}. The corresponding rate at sea level and high latitude is estimated at 48.8 ± 3.4 atoms (g Ca)$^{-1}$ a^{-1}. The muon capture rate used to derive these values is 8.8 ± 2.2 atoms (g Ca)$^{-1}$ a^{-1} at the Tabernacle Hill site, scaled from a value of 4.8 ± 1.2 atoms (g Ca)$^{-1}$ a^{-1} at sea level and high latitude. The calcium spallation rate determined in this study is in excellent agreement with previous whole-rock calibration measurements at Tabernacle Hill, when these are recalculated with respect to the absolute timescale.

The calibration of ^{36}Cl production from calcium underpins development of an exposure dating technique for calcite. Due to its high calcium content, the ^{36}Cl production rate in calcite is higher than in any other common rock-forming mineral. Measurement of ^{36}Cl in calcite, with an accelerator mass spectrometric detection limit of $\sim 5 \times 10^3$ atoms per gram, allows dating of limestone surfaces exposed for periods ranging from $\sim 10^2$–10^6 years. Alternatively, erosion rates from less than 1 to greater than 1000 μm per year can be determined in the case of eroding karst surfaces. Though the ^{36}Cl production rate is lower in calcium feldspar than in calcite, measurements on this mineral will provide a useful means of dating young basalt lavas.

1. INTRODUCTION

Dating geomorphic features has proved to be a major challenge in the study of landscape evolution. The problem has prompted novel applications of quantitative radiometric dating methods to materials such as rock-surface coatings and sedimentary deposits associated with landscape features. Other approaches have relied on relative measures of surface age, largely based on chemical and physical responses to weathering. During the past decade, the development of accelerator mass spectrometry (AMS) for analysis of isotopes such as ^{10}Be, ^{26}Al, and ^{36}Cl at ultra-low levels has given rise to dating methods based on the accumulation of these isotopes in rock surfaces exposed to cosmic radiation (Lal, 1988). Recent calibration studies of cosmogenic isotope production (Nishiizumi et al., 1989; Zreda et al., 1991), combined with extensive data on the cosmic ray flux and its variation over (and beneath) the Earth's surface (Lal and Peters, 1967; Lal, 1988), promise quantitative and widely applicable methods for studying the exposure of geomorphic surfaces. Cosmogenic isotope measurements have already been used to determine the exposure histories of features such as moraine boulders and glacial pavements, lava flows, shore platforms, alluvial fans, landslides, cliff surfaces, and meteorite impact deposits (Craig and Poreda, 1986; Kurz, 1986; Phillips et al., 1986, 1991; Klein et al., 1988; Cerling, 1990; Phillips et al., 1990; Nishiizumi et al., 1991a,b, 1993; Stone et al., 1995).

The sensitivity of an exposure dating method involving a particular cosmogenic isotope and target rock or mineral is governed by the production rate of the chosen isotope in the target, and the analytical sensitivity of the isotopic measurement. It will always be advantageous to work with an isotope whose analytical detection limit is low, and a target mineral in which the production rate of that isotope is high. These factors minimise the exposure time required to produce a measurable isotopic concentration, enhance the precision of the measurement, and reduce the required sample size. This consideration prompted us to explore the measurement of cosmogenic ^{36}Cl in calcite, to capitalise on the high sensitivity of chlorine isotopic analyses by AMS and the expectation (based on spallation systematics) of a high ^{36}Cl yield in calcite, due to its high calcium content. To obtain an accurate calibration of the ^{36}Cl production rate from calcium, the study was extended to include measurements of calcium feldspar from a well-dated basalt lava flow. The geological abundance of limestone suggests that measurements of cosmogenic ^{36}Cl in calcite will find widespread application in exposure dating and (where surfaces are eroding) the study of karst landform development. Measurements on Ca-rich minerals such as plagioclase and pyroxene in basic rocks should prove equally useful, for example, in dating basalts too young to be dated by the K-Ar and $^{40}Ar/^{39}Ar$ methods.

* *Present address:* Department of Medical Radiations Science, Royal Melbourne Institute of Technology, GPO Box 2476V, Melbourne, Victoria 3001, Australia.

Chlorine-36 measurements on calcite have been made previously by Kubik et al. (1984) who studied both "meteoric" ^{36}Cl in animal bones and ^{36}Cl produced in situ in a surficial limestone deposit. The present work also builds on developments by Phillips et al. (1986) who measured cosmogenic ^{36}Cl (produced in part from calcium isotopes) in whole-rock samples and Zreda et al. (1991) who sought to establish a quantitative basis for surface dating with ^{36}Cl by measuring its production rates in cosmic ray reactions with calcium, potassium, and ^{35}Cl in whole-rock samples. While whole-rock dating methods have the advantage of wider applicability than those restricted to particular minerals such as calcite or calcium feldspar, the sensitivity and simplicity of the methods described here should make them useful for precise surface dating.

This paper is the first of a pair describing the calibration of ^{36}Cl-producing reactions involving calcium over the depth range 0–20 m. This paper deals with ^{36}Cl production by calcium spallation and (to a lesser degree) by neutron capture on ^{35}Cl, the reactions of greatest importance at shallow depths. The second paper (J. M. Evans et al., unpubl. data hereafter Paper II) describes the production of ^{36}Cl by negative muon capture and reactions involving muon-produced secondary neutrons. These processes dominate production at depths beyond a few metres and are particularly important for estimating erosion rates from ^{36}Cl measurements. Unfortunately, space precludes publication of this entire body of work in a single paper. Separation of the two studies has little impact on the conclusions presented in this paper, however, since muon capture accounts for only ~6% of total production from calcium at the site used for the spallation calibration. Nevertheless, results from Paper II are provided in the discussion and calculations below, where required. An account of the preliminary work described in these papers was published in the Proceedings of the AMS-6 conference (Stone et al., 1994). The present, more detailed account is based on a larger set of samples and incorporates a revised calibration based on the absolutely dated Tabernacle Hill lava flow. The production rates presented here entirely supersede those given in the previous work.

This paper describes experimental methods used throughout the study and documents the overall reproducibility of exposure dates based on ^{36}Cl. It then presents a calibration of ^{36}Cl production and compares the rates derived, scaled to sea level and high latitude, to previous estimates. Aspects of cosmic ray physics and nuclear physics relevant to ^{36}Cl production and accumulation are discussed as required (here and in Paper II). More comprehensive reviews are provided by Lal and Peters (1967), Fabryka-Martin (1988), and Lal (1988).

2. ANALYTICAL METHODS

The chemical procedures used in this work follow well-established methods for separation and purification of AgCl (e.g., Conard et al., 1986). A brief summary is given below, concentrating on yields, blanks, and other aspects of note. Further details can be obtained from the first author.

2.1. Sample Preparation and Chloride Chemistry

To remove potential meteoric ^{36}Cl contamination, crushed samples were leached thoroughly, first in deionised water, then twice in 2% HNO_3. For calcite, sufficient acid was added to dissolve the outermost 10–15% of grain surfaces. Calcite was leached at room temperature, feldspar at 70–80°C. Calcite was selectively dissolved by gradual addition of 2 M HNO_3, keeping the overall acid strength of the sample solutions below 0.5 M. Calcium feldspars were dissolved over 2–3 days in a 15 M HF/2 M HNO_3 mixture at 60–70°C. Approximately 1 mg of chloride carrier was added to increase the final sample size and decrease the propagation of chloride concentration measurement errors into the calculation of ^{36}Cl concentrations. An optimum strategy would be to add carrier such that the ratio $(Cl_{carrier})/(Cl_{rock})$ matches the proportions of ^{36}Cl production from calcium and ^{35}Cl. At this ratio, error in the measurement of rock chloride propagates equally into the calculation of ^{36}Cl concentration and ^{36}Cl production rate, and therefore cancels in the estimate of exposure age. In this study, the amount of carrier added was typically 2–3× lower than the optimum to keep $^{36}Cl/Cl$ ratios high for the AMS measurements and to maintain some sensitivity to Cl concentration, allowing ^{36}Cl production by neutron capture to be calibrated.

Chloride was recovered from the sample solutions as AgCl, then redissolved in dilute NH_4OH. Sulphate coprecipitated with AgCl was then removed by precipitation of $BaSO_4$. Removal of sulphur is essential due to interference of isobaric ^{36}S with ^{36}Cl in the AMS measurements. Pure AgCl for AMS was reprecipitated by acidification, recovered, washed, dried, and packed into accelerator targets. Sample weights ranged from approximately 5 to 15 g while total chloride (including carrier) was typically in the range 1–2 mg, giving ~4–8 mg AgCl for analysis. Yields ranged from ~60% for 4 mg AgCl samples to >90% for the largest samples. Chloride blank from the total procedure was ~2–10 $\mu g\ Cl^-$, depending in part on the amounts of acid required for sample dissolution. Chlorine-36 blanks were measured with each batch of four to eight samples and averaged $(2.2 \pm 1.5) \times 10^4$ atoms over the course of the study.

2.2. Accelerator Mass Spectrometry

Chlorine isotopic ratios were measured with the 14-UD pelletron accelerator at the Australian National University (ANU) (Fifield et al., 1990, 1994). Samples of AgCl weighing ~ 1.5–2 mg (half of the AgCl recovered from the chemistry) were loaded and generally produced beam currents of 2–4 $\mu A\ ^{35}Cl^-$. Chlorine-36 was transmitted at a terminal voltage of 14 MV, and detected at 154 MeV in the 10+ charge state. Total instrumental efficiency (ions collected/atoms loaded) over the 30 min counting period was approximately $2–5 \times 10^{-4}$, giving 2–4 ^{36}Cl events at a $^{36}Cl/Cl$ ratio of 10^{-15}. Non-^{36}Cl background was ≤1 event in the ^{36}Cl region of the energy loss spectra over this period. Count rates of the ^{36}S isobar were generally below 200 Hz, though complete discrimination between ^{36}Cl and ^{36}S was maintained up to count rates of ~5 kHz.

Isotopic ratios were calculated directly from ion counts and integration of the stable isotope currents (without recourse to normalisation) though a working standard was run with every batch of twelve samples. Measurement uncertainties combine both ^{36}Cl counting statistics and the long-term reproducibility of the working standard (σ ~ 3.4% at the outset, presently ~2.8%). For samples with $^{36}Cl/Cl$ ratios less than $\sim 2 \times 10^{-13}$, counting statistics dominate the measurement uncertainty; above this ratio uncertainties approach the limit set by the day-to-day stability of the working standard.

2.3. Chloride Analyses

Two different methods were required to measure chloride concentrations in carbonate and silicate samples. In the case of calcite, chloride measurements were made by absorption spectrophotometry using the mercury (II) thiocyanate method (Florence and Farrar, 1971). Determinations were made in duplicate or triplicate and were assigned an uncertainty equal to the range of measurements on the splits. For most samples, errors better than ±2–3 ppm chloride in the parent rock were obtained. The detection limit for our implementation of the method is ~5 ppm chloride in rock. For silicates, chloride was measured by ion chromatography after stripping by pyrohydrolysis (Evans et al., 1981). Samples were mixed with V_2O_5, Cu, and Fe metal and heated to ~1400°C in an induction furnace under a

stream of H_2O-saturated oxygen. Volatile chlorine-bearing species evolved in this process were captured in a $Na_2CO_3/NaHCO_3$ buffer solution and analysed as chloride by ion chromatography. Yields for the procedure (ranging from ~80–95%) were monitored by standard addition and measurement of rock standards. For samples containing more than 20–30 ppm chlorine, the uncertainty attainable with our implementation of the method is ±10%, limited by the reproducibility of the chloride yield. For Cl-poor samples such as those measured in this study, detection limits and uncertainties are dictated by the size and reproducibility of blanks. Blanks from 2–5 μg chlorine were obtained with different batches of crucibles and reagents, permitting detection of chlorine at levels down to 2–4 ppm in rock.

At the outset of the study, chloride concentrations in calcite samples were measured on separate aliquots of rock, split after the leaching procedure and dissolved under the same conditions as the AMS samples. It was soon discovered that chloride measurements on calcite can vary according to crushing and leaching procedures, making subsampling a potential source of error. To overcome this problem, the AMS sample preparation procedure for calcite samples was modified by postponing carrier addition, allowing Cl to be measured on aliquots of the sample solutions being prepared for AMS. Thus far, comparable problems of heterogeneity have not been encountered with silicate samples. Chloride measurements on silicates for this study were therefore made on rock aliquots after the complete leaching procedure.

2.4. Ancillary Chemical Analyses

To reconstruct the target chemistry of carbonate samples, calcium, magnesium, and iron concentrations were measured by inductively coupled plasma (ICP) optical emission spectrometry in aliquots of the AMS sample solutions. The mean difference between duplicate calcium concentrations measured in this way was <0.3%. Calcium and potassium in feldspar samples were measured by X-ray fluorescence (XRF) with relative uncertainties better than ±1%.

To determine ^{36}Cl production rates from neutron capture by ^{35}Cl, macroscopic cross sections ($=\Sigma\sigma_i N_i$, where σ_i is the neutron-capture cross section of nuclide i, with abundance N_i) were calculated from whole-rock chemical compositions (Davis and Schaeffer, 1955). Major element concentrations were measured by XRF (or estimated from the composition of the carbonate phase and the mineralogy of the insoluble fraction, determined by X-ray diffraction, in the case of some carbonate samples). Trace neutron absorbers were measured either by ICP (B) and neutron activation (Sm, Gd), or together by inductively coupled plasma–mass spectrometry (ICP–MS). Concentrations of the trace absorbers were found to be low in the carbonate samples, B averaging 2.5 ppm, Sm 0.9 ppm, and Gd 0.7 ppm. Maximum values were 6 ppm B, 1.7 ppm Gd, and 2.3 ppm Sm.

Calcium is the principal neutron absorber in all of the carbonate samples. The macroscopic cross section of the Tabernacle Hill basalt is higher than those of the limestones, reflecting higher Fe, Gd (4.3 ppm), and Sm (4.7 ppm) contents. Uranium and thorium concentrations required to estimate background concentrations of ^{36}Cl produced by capture of fission and (α, n) neutrons were measured by ICP–MS.

3. ANALYTICAL RESULTS—TRIALS AND VALIDATION OF THE METHOD

3.1. Analytical Reproducibility

The ultimate precision of exposure ages measured with the method described here depends on the combined uncertainties of the ^{36}Cl, chlorine, calcium, and neutron absorber analyses. Our most recent measurements have yielded exposure ages with fully propagated uncertainties (not including uncertainties and systematic errors in production rates) approaching ±4% (1σ). This level of internal precision can be compared to the overall reproducibility of the method by examining replicate analyses. These comprise:

1) Measurements of five Ca-feldspar separates from three samples of the Tabernacle Hill basalt used to calibrate surface ^{36}Cl production (section 4 below).
2) Eight measurements of the three marble samples from Tioga Pass in the Sierra Nevada, California, USA, used for trial measurements of ^{36}Cl in calcite (section 5 below). In addition to duplicate 125–250 μm fractions of all three samples, separate subsamples of SGP-3 and SGP-4 were analysed as crushed (predominantly <125 μm material).
3) A surface limestone sample from the Cooleman Plain, in the Snowy Mountains of southeastern Australia, analysed by stepwise dissolution to check for ^{36}Cl retention by calcite.

Results of these analyses can be found in Tables 2, 5, and 1, respectively. Uncertainties are quoted at the 1σ (68% confidence) level, and include all known analytical errors, blanks and background effects. The agreement among duplicate ^{36}Cl results (after correction to common chloride concentrations, to allow for differences in production via ^{35}Cl) is entirely consistent with their statistical uncertainties. The standard deviation of the Tabernacle Hill feldspar measurements, obtained from AgCl loads containing approximately 10^6 atoms of ^{36}Cl, is ±3%. Successive dissolution steps of the Cooleman Plain limestone sample, from which 2–4 × 10^6 atoms of ^{36}Cl were loaded for measurement, give a standard deviation of ±2.1%.

It will be noted from the comparison above that differences in chloride concentration (far in excess of analytical uncertainty) were found between duplicates of several of the carbonate samples pretreated in different ways. The most extreme example is SGP-4, for which splits of the unsieved (predominantly fine-grained) sample SGP-4/1 gave 37 and 41 ppm Cl, while triplicate measurements of the sieved (125–250 μm) sample SGP-4/2 gave 12.8, 13, and 13.7 ppm. Checks on the procedure, including measurements by standard addition and gravimetry, indicate that these differences are real and must be explained in terms of heterogeneity of the original rock samples and/or differences in their response to crushing and leaching. As chlorine is not a lithophile element and is unlikely to occupy a carbonate lattice site, its concentration may be determined by features such as fluid inclusions, veins, grain overgrowths, and recrystallised calcite, which may respond differently to crushing and leaching procedures. As discussed above, the possibility of errors arising from differences in chloride between the rock processed for ^{36}Cl and chloride measurements is easily eliminated, by taking aliquots from the AMS sample after dissolution. Errors in the calculation of ^{36}Cl concentration arising from errors in chloride measurement are also suppressed by the addition of chloride carrier.

3.2. Closure of Calcite to ^{36}Cl Exchange

If calcite is to be used for exposure dating, it is important to ensure that its solubility in natural waters, combined with the hydrophilic behaviour of chlorine, do not lead to loss of ^{36}Cl produced in situ or to uptake of meteoric ^{36}Cl. A clear distinction between internally and externally produced ^{36}Cl is

Table 1. Stepwise dissolution of Cooleman Plain limestone [1]

Step	Weight loss [2] (g)	Cumulative fraction dissolved [2] %	[Ca] (g g^{-1} in calcite)	[Cl] (μg g^{-1} in calcite)	$\sigma_{35}N_{35}$ / $\Sigma\sigma_i N_i$ [3]	[^{36}Cl] [4] (10^6 atoms g^{-1})
Leach 1	1.610	8.0	0.398 ± 0.001	6.5 ± 1.0	Not	1.26 ± 0.10
Leach 2	1.902	17.5	0.398 ± 0.001	4.8 ± 1.4	measured	1.52 ± 0.11
Dissolution 1	4.083	37.8	0.398 ± 0.001	7.4 ± 1.2	on	1.48 ± 0.07
Dissolution 2	4.030	57.9	0.398 ± 0.001	5.1 ± 0.7	individual	1.48 ± 0.08
Dissolution 3	4.044	78.1	0.398 ± 0.001	8.6 ± 1.2	fractions	1.42 ± 0.07
Dissolution 4	4.399	100%	0.398 ± 0.001	8.8 ± 1.6		1.47 ± 0.07
Composite of dissolution steps	-	-	0.398 ± 0.001	7.5 ± 0.6	0.00149 ± 0.00011	1.46 ± 0.04
Standard method[5]	6.396	-	0.398 ± 0.001	5.1 ± 1.0	0.00101 ± 0.00020	1.41 ± 0.05

[1] Site and sample details: Cooleman Plain: 148° 39' E 35° 36' S, elevation 1285 m. Thickness 13 g cm^{-2}. Unobstructed 2Π exposure geometry.

[2] Weights based on calcite dissolved. Sample is < 1% insoluble material.

[3] Based on effective neutron absorption cross sections. Uncertainties reflect analytical errors (cross section uncertainties not propagated).

[4] Cosmogenic ^{36}Cl, after subtraction of U-fission, (α,n) -produced ^{36}Cl. Corrections are < 0.1%. Uncertainties are ± 1σ including blank corrections, [Cl] and AMS errors.

[5] Approximately 15% leached prior to dissolution.

required, since cosmic rays produce 3–6 × 10^4 atoms ^{36}Cl cm^{-2} a^{-1} in traversing the atmosphere (Lal and Peters, 1967; Bentley et al., 1986), roughly 10 times their yield in calcite below ground. Rainfall delivers this meteoric component, accompanied by stable chloride, at ^{36}Cl/Cl ratios ranging from ~10^{-15} near coasts up to ~10^{-12} inland. Since these ratios can be higher or lower than intrinsic ^{36}Cl/Cl in calcite, contamination by meteoric chloride could result in erroneously high apparent exposure ages (where the meteoric contaminant is rich in ^{36}Cl) or erroneously low ages (where contamination increases the apparent chloride content of the rock).

The solubility of chloride and the utility of ^{36}Cl as a tracer in groundwater suggest that meteoric chloride and ^{36}Cl are unlikely to be tenaciously bound to grain surfaces. Nonetheless, a sequential dissolution experiment was carried out to test our leaching procedure for removal of meteoric ^{36}Cl, and to confirm that ^{36}Cl produced in situ remains firmly bound within the calcite lattice. A sample of limestone from the Cooleman Plain in southeastern Australia, an area of comparatively rapid surface erosion (20–30 μm a^{-1}; Stone et al., 1994), was chosen to maximise the likelihood of detecting any ^{36}Cl loss. In addition the low chloride content of the test sample should highlight the presence of any meteoric chloride contamination.

The stepwise dissolution experiment was carried out on 20.25 g of sample, crushed, and sieved to 150–250 μm, avoiding all contact with water. Note that this contrasts with the normal preparation procedure, in which sample surfaces would be sawn or ground clean under a stream of cooling water, then wet-sieved and washed free of fine material prior to leaching. Dissolution was broken into six stages by administering fixed quantities of dilute acid. After complete reaction at each step, the dissolved $Ca(NO_3)_2$ was collected and split for chloride and AMS measurements and the residual solid rinsed, dried, and weighed. Results are given in Table 1 and the stepwise ^{36}Cl release pattern is shown in Fig. 1.

After the first leaching step, ^{36}Cl release occurs at a constant concentration of 1.46 ± 0.04 × 10^6 atoms g^{-1}, in very good

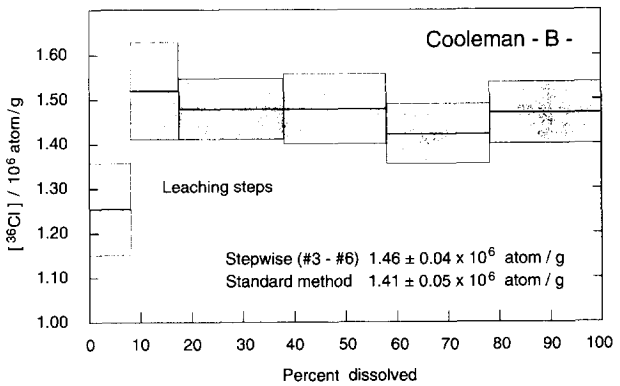

FIG. 1. Chlorine-36 concentrations in successive leach and dissolution steps of Cooleman Plain limestone, as discussed in section 3.2 of text. Error limits are ±1σ.

agreement with a separate measurement of the same material prepared with the standard leaching and dissolution procedure, of $1.41 \pm 0.05 \times 10^6$ atoms g^{-1}. There is no sign of contamination by meteoric chloride in the initial leaching steps. The low ^{36}Cl content of the first leaching step, which would be discarded in the normal pretreatment, is presumably due to slight depletion of the in situ produced isotope by natural dissolution of grain surfaces. In summary, it appears that contamination residing within the dry rock at the time of sampling cannot amount to more than a few μg of chloride per gram of rock, and that the leaching procedure guarantees the integrity of the calcite analysed for in situ ^{36}Cl. There is no evidence that dissolution under natural conditions leads to ^{36}Cl loss from deep within the mineral lattice, even under the high erosion rate experienced by the test sample.

3.3. Chloride Yields and Carrier Equilibration

While investigating methods for dissolution of silicate samples it was found that the use of concentrated HNO_3 can lead to oxidation of Cl^-, followed by loss of volatile Cl_2. Since stable chloride and ^{36}Cl occupy different sites in the sample and therefore enter solution at different stages of the digestion, and since carrier is added either before or after dissolution, any chloride loss during the procedure could skew the final isotopic ratio. To ensure isotopic equilibration as chloride, the extraction methods adopted never expose samples to HNO_3 strengths greater than ~2 M for silicates or ~0.5 M for carbonates, with negligible oxidising power. To confirm the retention of chloride during this procedure, sieved fractions of three calcite samples from the Sierra Nevada were split and one set spiked with carrier prior to, the other after, dissolution. The ^{36}Cl concentrations in Tables 1 and 2 show no systematic differences between the paired samples, and agree within their statistical uncertainties (and in the case of SGP-3 and SGP-4, with other measurements of the same parent material). Together with the overall level of analytical reproducibility documented above, this is taken to indicate that carrier, sample chlorine and sample ^{36}Cl achieve chemical and isotopic equilibrium as dissolved chloride, and are fully retained in solution. Chloride losses (indicated by the final yields of AgCl) are therefore inferred to occur during later stages of the chemical separation, especially in the final AgCl precipitation and recovery.

3.4. Detection Limits

Complete procedural blanks prepared and run with each batch of samples averaged $(2.2 \pm 1.5) \times 10^4$ atoms ^{36}Cl. Eleven blanks were run over the course of this study, ranging from $(0.7 \pm 0.7) \times 10^3$ atoms to $(5.0 \pm 2.8) \times 10^4$ atoms. These values give an isotopic ratio relative to the stable chloride blank of $\sim 3 \times 10^{-13}$, similar to Canberra rainfall. Likely sources of blank are therefore aerosols and laboratory personnel rather than reagent impurities, which would be expected to have an "industrial" (seawater) chloride isotopic composition of $\sim 10^{-15}$.

As the blank measurements, which typically yield 1–3 ions during the counting period, fall close to the detection limit of the AMS system, their individual uncertainties are large, and definition of a "detection limit" becomes fairly arbitrary. We believe that under typical preparation and measurement conditions, 10^5 atoms of ^{36}Cl (equal to twice the worst-case blank, and corresponding to a $^{36}Cl/Cl$ ratio of $\sim 5 \times 10^{-15}$) can be unequivocally distinguished from the analytical blank and measured with a fully propagated uncertainty better than ±50%. For a maximum sample size of 20 g, the corresponding detection limit is approximately 5×10^3 ^{36}Cl atoms per gram. There is scope for improving this simply by increasing sample sizes, reducing the addition of carrier and extending the 30 min counting times presently used for sample and blank analyses. Duplicate measurements of deep limestone samples to be presented in Paper II show that reproducible analyses

Table 2. Tabernacle Hill feldspar samples [1]

Sample [2]	Weight (g)	[Ca] ($g\ g^{-1}$)	[K] ($g\ g^{-1}$)	[Cl] ($\mu g\ g^{-1}$)	$\sigma_{35}N_{35}$ / $\Sigma\sigma_i N_i$ [3]	$[^{36}Cl]$ [4] (atoms g^{-1})
TH-1f	4.686	0.0928 ± 0.0009	0.0020 ± 0.0001	3 ± 1	0.00025 ± 0.00008	(2.85 ± 0.16) x 10^5
TH-2f	7.316	0.0949 ± 0.0009	0.0019 ± 0.0001	2 ± 1	0.00020 ± 0.00007	(2.73 ± 0.11) x 10^5
TH-2c	10.209	0.0949 ± 0.0009	0.0019 ± 0.0001	5 ± 1	0.00042 ± 0.00009	(2.70 ± 0.12) x 10^5
TH-3f	7.815	0.0936 ± 0.0009	0.0019 ± 0.0001	4 ± 1	0.00033 ± 0.00009	(2.64 ± 0.11) x 10^5
TH-3c	9.056	0.0936 ± 0.0009	0.0019 ± 0.0001	3 ± 1	0.00024 ± 0.00008	(2.68 ± 0.11) x 10^5

(1) Tabernacle Hill: Geographic latitude: 38° 56' 05" N. Effective geomagnetic latitude 40.9° over 17.3 ka. Elevation 1445 m. Scaling factor to sea-level and high latitude for spallation and spallogenic neutron production: 3.114. Scaling factor for muon capture reactions: 1.832. All samples exposed with unobstructed 2Π geometry. Sample thicknesses: TH-1: 13 g cm^{-2}, TH-2: 12 g cm^{-2}, TH-3: 15 g cm^{-2}. Thickness corrections of 0.960, 0.963, and 0.950 applied to surface spallation rate for these samples respectively.

(2) "f" denotes 125 - 250 μm size fraction. "c" denotes 250 - 500 μm size fraction.

(3) Based on effective neutron absorption cross sections. Uncertainties reflect analytical errors (cross section uncertainties not propagated).

(4) Cosmogenic ^{36}Cl. U-fission and (α,n) neutron-produced ^{36}Cl negligible (< 100 atom g^{-1}). Uncertainties are ± 1σ including blank corrections, [Cl] and AMS errors.

with ±10–15% precision can be achieved at levels of ~5 × 10^4 atoms g^{-1}, roughly 10× the assumed detection limit.

4. CALIBRATION OF CHLORINE-36 PRODUCTION BY CALCIUM SPALLATION

4.1. Near-Surface Chlorine-36 Production in Ca-Rich Minerals

The principal source of ^{36}Cl in Ca-rich minerals is spallation of calcium isotopes by fast cosmic ray nucleons. Capture of cosmic ray negative muons via the reaction $^{40}Ca(\mu^-, \alpha)^{36}Cl$ is a minor source of production from calcium at the surface, but becomes predominant at depths below a few metres. The measurements described here and to be presented in Paper II (see also Stone et al., 1994) allow separate calibration of these two Ca-dependent reactions, using samples from different altitudes and depths to discriminate between production by the nucleon and muon fluxes. High Ca/Cl and Ca/K ratios in the calcium feldspar samples used to calibrate the calcium spallation rate make the result insensitive to other ^{36}Cl-producing reactions.

In rocks and minerals containing significant amounts of chlorine, thermal neutron capture by ^{35}Cl is a third source of cosmogenic ^{36}Cl. At ground level and depths down to a couple of metres, most neutrons are the secondary products of spallation and muon capture reactions within (and above) the rock surface. Spontaneous fission of ^{238}U and (α, n) reactions support a constant, noncosmogenic "background" neutron flux within the rock, though low uranium and thorium concentrations in limestone and basalt (typically <1 ppm) and low concentrations of light elements such as fluorine, sodium, and magnesium in many limestones generally render this source negligible. After thermalisation, neutrons are captured by isotopes in the rock including ^{35}Cl; hence, the ^{36}Cl production rate is given by the product of the total neutron capture rate and the abundance-weighted cross section of ^{35}Cl relative to other neutron absorbers in the rock (Davis and Schaeffer, 1955). The total cosmogenic neutron-capture rate has been measured for rocks of granitic composition (Zreda et al., 1991). Different neutron-capture rates will occur in other rock types due to the compositional dependence of secondary neutron yields and the sensitivity of the thermal neutron flux to sample thickness, exposure geometry, and water content (O'Brien et al., 1978; Dep et al., 1994). The low chlorine concentrations of feldspar samples used for calibration in this study make the results insensitive to details of neutron production and capture. Measurements on calcite presented in section 5 provide an independent, though imprecise, estimate of the near-surface neutron-capture rate in limestone, however.

4.2. Calibration Strategy

Though significant advances have been made in calculating cosmogenic nuclide production rates (e.g., Masarik and Reedy, 1995), rates based on nuclide concentrations in geomorphic surfaces offer a sense of "ground truth." Accurate rates can only be derived, however, from continuously exposed surfaces which have been accurately and independently dated. Independent ages based on radiocarbon dating must be corrected to siderial timespans (in "absolute," "calibrated," or "cal." years) to avoid introducing an error from the offset between "radiocarbon" and absolute timescales.

With these considerations in mind, we chose to base our calibration of near-surface ^{36}Cl production on the Tabernacle Hill basalt flow in Utah, USA. The altitude of the site ensures an enhanced production rate and decreases sensitivity to muon contributions, which diminish relative to production by fast nucleons with increasing altitude. Production by muon capture in the calibration samples is approximately 6% of the calcium spallation rate, making the spallation calibration insensitive to error in the muon capture rate. To minimise corrections for other ^{36}Cl-producing reactions and avoid cumulative errors in the calcium calibration, calcium feldspar was separated from the basalt samples. Ca/K and Ca/Cl ratios in the feldspars are approximately 4 and 40 times higher, respectively, than in whole-rock samples of the Tabernacle Hill basalt used by Zreda et al. (1991) to calibrate the calcium production rate (see section 4.6 below). The low Cl/Ca ratio of the feldspars minimises sensitivity to uncertainty in the cosmogenic neutron-capture rate and to ^{36}Cl background from noncosmogenic neutrons. Levels of "background" ^{36}Cl supported by ^{238}U fission and (α, n) reactions in the samples are $<10^2$ atoms g^{-1} (calculated as per Fabryka-Martin, 1988), compared to ~2.7 × 10^5 atoms g^{-1} from calcium reactions.

4.3. Site and Sample Details

The Tabernacle Hill basalt was chosen for the calibration because of closely bracketing radiocarbon dates and excellent surface preservation. Samples from this flow have been used previously to calibrate ^3He production in olivine (Cerling, 1990) and ^{21}Ne production in feldspar (Poreda and Cerling, 1992). Zreda et al. (1991) measured whole-rock samples of the basalt to calibrate ^{36}Cl production from calcium. In this study, plagioclase feldspar was separated for analysis to obtain material with the highest possible calcium concentration, Ca/K, and Ca/Cl ratios. Full geographic details of the site and all correction factors used to normalise production rates to reference values (i.e., surface rates at sea-level and latitudes > 60°) are listed in Table 2.

The Tabernacle Hill basalt was erupted onto the Provo shoreline of the Lake Bonneville basin, cut after catastrophic lowering of the lake in the Bonneville flood (Oviatt and Nash, 1989). The age of the flood is tightly constrained by radiocarbon dates at 14.5 ka on the ^{14}C-timescale. This is therefore an upper bound on the age of the lava. Pillow structures and tufa deposits associated with the basalt indicate that it flowed into Lake Bonneville during the Provo stand, or before the lake had fallen more than a few metres below the Provo level, which persisted until ~14.3 ka on the ^{14}C-timescale. This sets a lower bound on the age of the basalt, confirmed by a further radiocarbon date of 14.3 ± 0.1 ka on encrusting tufa (Oviatt and Nash, 1989). The age of the Tabernacle Hill basalt is therefore taken as 14.4 ± 0.1 ka in the radiocarbon timescale. This corresponds to an absolute age of 17.3 ± 0.3 ka (Stuiver and Reimer, 1993), based on the most recent data of Bard et al. (1993). Note that this age is ~3% younger than the value

of 17.8 ka used by Poreda and Cerling (1992) in their study of ^{3}He and ^{21}Ne production rates, which was based on an earlier calibration of the ^{14}C timescale (Bard et al., 1990). Since the updated calibration contains little new data in the relevant part of the timescale, it seems prudent to assign a larger uncertainty to the absolute age of the basalt, which we therefore take as 17.3 ± 0.5 cal. ka.

Samples with well preserved pahoehoe surface textures were collected to guarantee zero erosion. Two samples were obtained from the tops of steep-sided pressure ridges, to ensure rapid removal of ash associated with the eruption. The third sample (TH-3), though collected from a gently dipping flow surface, gives an indistinguishable exposure age, which is taken to preclude thick or prolonged shielding by ash (the post-basaltic Tabernacle Hill ash forms a layer up to 70 cm thick in surrounding lake sediments, but is not preserved on the flow surface). As further confirmation of the flow's continuous exposure, Cerling (1990) showed that cosmogenic ^{3}He measurements calibrated with respect to the flow correctly date a boulder transported by the Bonneville flood. This more stringent consistency test would not be satisfied if the exposure time of the flow had been reduced by ash cover.

4.4. Calibration Results

Full analytical results for the Tabernacle Hill samples are presented in Table 2, and ^{36}Cl concentrations are shown in Fig. 2. The figure also shows concentrations normalised to uniform composition and thickness, allowing purely Ca-derived ^{36}Cl concentrations to be compared.

Chlorine-36 production rates in the feldspar samples depend on their calcium, potassium, and chlorine contents;

$$P = P_{Ca}[Ca] + P_{K}[K] + \psi_n(\sigma_{35}N_{35}/\Sigma\sigma_i N_i), \quad (1)$$

where P_{Ca} and P_{K} are production rates for reactions on calcium and potassium, respectively, [Ca] and [K] denote element concentrations and ψ_n is the thermal neutron-capture rate (in units of neutrons absorbed g^{-1} a^{-1}). The $(\sigma_{35}N_{35}/\Sigma\sigma_i N_i)$ term gives the fraction of stopped neutrons captured by ^{35}Cl, determined by effective cross sections (σ_i) and abundances (N_i) (Davis and Schaeffer, 1955). Neutron absorption by the non-1/v absorbers gadolinium and samarium is treated using the effective cross-section formalism of Lingenfelter et al. (1972). The value of P_{Ca} includes production both by calcium spallation and muon capture on ^{40}Ca. Separation of these components requires subtraction of the muon capture rate, which is estimated at 8.8 ± 2.2 atoms g^{-1} a^{-1} at the Tabernacle Hill site (Paper II, slightly revised from Stone et al., 1994). Due to the low potassium and chlorine contents of the feldspar samples, production from these elements contributes little ^{36}Cl. The production rate for potassium reactions at Tabernacle Hill is taken as 590 atoms (g K)$^{-1}$ a^{-1}, derived by scaling the potassium rate at sea level and high latitude (190 atoms (g K)$^{-1}$ a^{-1}; Zreda, 1994; Swanson et al., 1994; and unpublished ANU data) to 1445 m at an effective geomagnetic latitude of 40.9° (see section 4.5 below). The production rate by thermal neutron capture assumes $\psi_n = 900n$ g^{-1} a^{-1}, scaling the sea level/high latitude value of $\psi_n = 307n$ g^{-1} a^{-1} (Zreda et al., 1991) with the assumption that 80% of stopped neutrons at sea level are spallation secondaries and 20% muon-capture secondaries. This breakdown is based on a calibration of the secondary neutron yield from muon capture reactions, which indicates a production rate of seventy muon-induced neutrons g^{-1} a^{-1} at sea level and high latitude, 20% of the total neutron stopping rate (Paper II, slightly revised from Stone et al., 1994). From the compositional data given in Table 2 it can be seen that potassium reactions account for only 7% and neutron capture only 1–2% of the total ^{36}Cl in the samples. The calibration of P_{Ca} is therefore insensitive to any errors in the values assigned to P_{K} and ψ_n.

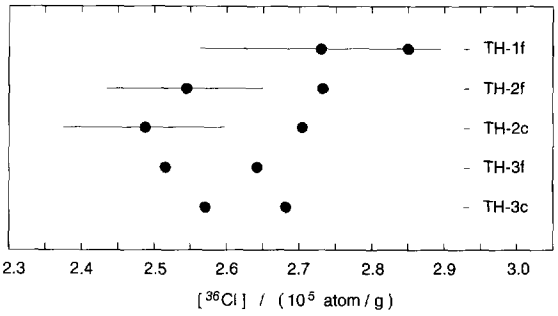

FIG. 2. Chlorine-36 concentrations in Tabernacle Hill feldspar samples. Light symbols are measured concentrations. Dark symbols with ±1σ error limits are for comparison on a common basis, after (1) subtraction of ^{36}Cl due to K spallation (7%), (2) subtraction of n-produced ^{36}Cl (1–2%), (3) normalisation to common Ca (set to Ab_{36} composition; 13.2 wt% CaO) (0–2%), and (4) correction to zero thickness (4–5%).

The value of P_{Ca} is calculated by a standard χ^2 fitting procedure, minimising the sum of inverse-error-weighted differences between measured ^{36}Cl concentrations and those calculated in terms of the "grow-in" equation:

$$N_{36,calc}(t) = (P/\lambda_{36})(1 - \mathrm{Exp}(-\lambda_{36}t)), \quad (2)$$

where λ_{36} is the ^{36}Cl decay constant equal to 2.303 × 10^{-6} a^{-1}, t the exposure age, and P the total production rate given by Eqn. 1. From the χ^2 calculation, the best estimate of P_{Ca} at the Tabernacle Hill site is 161 ± 11 atoms (g Ca)$^{-1}$ a^{-1} (Table 3.1). Subtracting the muon capture rate noted above gives a value of 152 ± 11 atoms (g Ca)$^{-1}$ a^{-1} for production by calcium spallation alone. This value is calculated for production at the air-rock interface, assuming an exponential decrease (with attenuation length 160 g cm^{-2}) through the 12–15 g cm^{-2} thick samples used for the calibration. Note, however, that recent radiation transport calculations by Masarik and Reedy (1995) suggest a constant spallation rate through the topmost ~ 12 g cm^{-2} of rock. In this case, the spallation rate given above would be reduced by ~4%. If the rate given here is applied to samples of 12–15 g cm^{-2} thickness, using the assumption of exponential depth-dependence to calculate a thickness correction, this factor will cancel out in exposure age calculations.

The uncertainties stated above are 95% confidence limits, derived from a 400 point Monte-Carlo error propagation including the full analytical uncertainties shown in Table 2, an uncertainty of ±0.5 ka in the age of the flow, uncertainties of ±20% in P_{K}, ψ_n and ±25% in the rate of the ^{40}Ca(μ^-, α)^{36}Cl

Table 3 — Calibrated chlorine-36 production from Ca (2Π surface rates)

Table 3.1 — Production rates from Ca

	P_{Ca} [1] (atoms g Ca^{-1} a^{-1})	$P_{40Ca(\mu^-,\alpha)36Cl}$ [2] (atoms g Ca^{-1} a^{-1})	$P_{Ca\text{-spallation}}$ (atoms g Ca^{-1} a^{-1})	Confidence interval 68%	95%
At Tabernacle Hill	161 ± 11	9 ± 2	152	± 5	± 11
At sea-level / λ > 60°	53.6 ± 3.6	4.8 ± 1.2	48.8	± 1.7	± 3.4

(1) Total of Ca spallation and $^{40}Ca(\mu^-, \alpha)^{36}Cl$ reactions.

(2) Derived from ^{36}Cl profile in limestone (Stone et al., 1994, and Paper II) scaled for altitude and latitude as described in text.

Table 3.2 — Production ratios in Tabernacle Hill minerals [1]:

P_{36Cl} (feldspar) / P_{3He} (olivine)	0.049 ± 0.004
P_{36Cl} (feldspar) / P_{21Ne} (olivine)	0.132 ± 0.013
P_{36Cl} / P_{21Ne} (feldspar)	0.333 ± 0.073

(1) Based on ^3He and ^{21}Ne data of Poreda and Cerling (1992). Chlorine-36 results corrected to zero Cl in feldspar. Calculated to weight ratio of target minerals. Average feldspar composition at Tabernacle Hill is 13.2% CaO + 0.23% K_2O (Ab_{36}). Olivine composition is Fo_{81}.

reaction. Limits for 68% confidence (the level typically quoted with AMS measurements) are ±5 atoms (g Ca)$^{-1}$ a^{-1}.

In contrast to production rates, isotope production ratios derived from natural surfaces are largely independent of errors in surface age and immune to past changes in the cosmic ray flux. Once calibrated, these ratios can be useful for constraining complicated exposure and erosion histories (e.g., Klein et al., 1988, 1993; Lal, 1991; Nishiizumi et al., 1991a). Isotopes such as ^{10}Be and ^{41}Ca are produced in situ in minerals such as calcium feldspar and calcite, ^{21}Ne is produced from sodium and aluminium in feldspar and there are situations in which other isotopes such as ^3He can be measured in coexisting minerals in a rock surface. The results given in Table 3.1 can be combined with the ^{21}Ne and ^3He concentrations measured by Poreda and Cerling (1992) to derive the production ratios for mineral targets shown in Table 3.2. The high production rate of ^3He in olivine compared to ^{36}Cl in feldspar is not surprising, since spallation of all elements yields ^3He (and ^3H) whereas ^{36}Cl is produced from calcium alone (4.9 atom % in Tabernacle Hill feldspar). The difference between the production rates of ^{21}Ne in olivine and ^{36}Cl in feldspar can be accounted for by the fivefold higher abundance of magnesium in olivine compared to calcium in feldspar (on an atoms cm^{-3} basis) with a ~50% higher spallation yield for the Ne-producing reaction. It should be noted that the values in Table 3.2 apply to specific mineral compositions and must be scaled if used for minerals of different composition. The production ratios also apply to an altitude of 1445 m and will differ slightly at other elevations according to the contribution of muon reactions to production of the three isotopes (see section 4.5 below).

4.5. Reference Production Rates at Sea Level and High Latitude

The calcium spallation rate at sea level and high latitude derived from the Tabernacle Hill data is 48.8 ± 3.4 atoms (g Ca)$^{-1}$ a^{-1} (Table 3.1). The procedure used to scale the spallation rate is based on the polynomials of Lal (1991) for cosmic-ray-induced disintegrations in air. The muon capture reaction rate is corrected for altitude using an attenuation length of 247 g cm^{-2} for the slow muon flux in the atmosphere (Conversi, 1950; Winsberg, 1956) and for latitude assuming the same sea level variation as for nucleons (cf. Lal, 1991; Nishiizumi et al., 1989).

To obtain production rates at high latitude which are independent of geomagnetic fluctuations during the calibration exposure, the results have been scaled with respect to the effective geomagnetic latitude of the Tabernacle Hill site, averaged over the past 17.3 ka. Our calculation of effective latitude (λ_{eff}) is similar to that described by Nishiizumi et al. (1989) and recently discussed by Clark and Bierman (1995). We use the relation

$$\mathrm{Cos}\,(\lambda_{eff,t}) = (M_t/M_0)^{1/4}\,\mathrm{Cos}\,(\lambda_0), \qquad (3)$$

where λ_0 and $\lambda_{eff,t}$ are latitudes in a centred dipole field of strength M_0 and M_t, at present and at time t, as denoted by the subscripts. Values of M_t were obtained from the palaeointensity data of McElhinny and Senanayake (1982) and Meynadier et al. (1992) and averaged over the exposure time, weighting intensity at time t by $e^{-\lambda_{36}t}$ to allow for ^{36}Cl decay since production. The dipole intensity of the magnetic field over the past 17.3 ka was slightly lower, on average, than its

present value, resulting in higher cosmogenic nuclide production rates at low latitude. To determine the calcium spallation rate at high latitude (which would not have experienced any corresponding enhancement) the results from Tabernacle Hill have been scaled with respect to an effective geomagnetic latitude of 40.9°, rather than the site's geographic latitude of 38.9°. The difference in scaling factors is ~4%.

4.6. Comparison with Previous Production Rate Estimates

Several previous estimates of ^{36}Cl production in calcite and other Ca-rich targets have been made. Comparisons between these and the present results are complicated by differences in the sites and exposure periods used for empirical calibrations, and differences in the altitude and latitude scaling procedures adopted. To allow comparison, the primary results of previous studies—production rates at particular sites, based on measured ^{36}Cl concentrations and chemical data—have been recalculated to sea level and high latitude. Production rates above the cosmic-ray "knee" at 50–60 degrees geomagnetic latitude (2–3 GV cut-off rigidity) are not significantly affected by fluctuations in the strength of the magnetic field, making values scaled to high latitude suitable for intercomparison. Production rates calibrated at lower latitudes will have been influenced by fluctuations in the dipole strength, however. To overcome this, rates have been recalculated by scaling to effective geomagnetic latitude, as described in section 4.5. Where necessary, previous estimates have also been broken down into spallation and muon-produced components, following the same procedures used in this work. The comparisons are shown in Table 4.

In an early study, Yokoyama et al. (1977) measured the activation of ^{22}Na and ^{24}Na by cosmic rays at Mt. Blanc and combined these results with reaction cross-sections to calculate production rates for other isotopes and target compositions, including ^{36}Cl in calcite. The production rate estimated for calcium spallation was 0.84 ± 0.17 atoms (kg calcite)$^{-1}$ min^{-1}, equivalent to 1100 ± 220 atoms (g Ca)$^{-1}$ a^{-1}. This is 30% higher than the rate derived in this work (790 ± 55 atoms (g Ca)$^{-1}$ a^{-1}) scaled to the same altitude and latitude. The discrepancy is not surprising, given that Yokoyama et al. (1977) had to assume cross sections for two separate reactions to arrive at their estimate. Agreement with the results of this study is probably better than the direct comparison indicates, since the samples measured by Yokoyama et al. (1977) were activated under conditions approaching solar minimum, exposing them to a higher-than-average cosmic ray flux.

The results of this study can be compared directly to the work of Zreda et al. (1991) who used basalt whole-rock samples from the Tabernacle Hill flow to calibrate ^{36}Cl production from calcium reactions. With the same assumptions used by Zreda et al. (1991), production rates of 229 and 259 atoms (g Ca)$^{-1}$ a^{-1} at Tabernacle Hill are obtained from the two samples measured in their study. For comparison, these rates must be recalculated using the exposure age and revised production rate from potassium set out in sections 4.3 and 4.4. This leads to calcium production rates of 149 and 179 atoms (g Ca)$^{-1}$ a^{-1}. Although the reason for the difference between the samples remains unclear, the average of 164 atoms (g Ca)$^{-1}$ a^{-1} is in excellent agreement with the rate of 161 atoms (g Ca)$^{-1}$ a^{-1} determined in this work.

The ~30% reduction in the original estimate of the calcium production rate of Zreda et al. (1991) results from the ~17% lag between "radiocarbon" and siderial time at 17 cal. ka and their underestimate of the amount of ^{36}Cl in their samples due to potassium spallation. With ~1% K_2O in the whole-rock samples, revision of the potassium spallation rate (at sea level and high latitude) to 190 atoms (g K)$^{-1}$ a^{-1} from its earlier value of 107 atoms (g K)$^{-1}$ a^{-1} (Zreda, 1993, and unpublished ANU data) reduces by a further 12–16% the fraction of ^{36}Cl in the rocks which can be ascribed to calcium production. These revisions illustrate the importance of using absolute surface ages to determine production rates, and the advantages of calibration samples in which production is dominated by a single target element. The close agreement

Table 4. Common-basis comparison between production rates

Study	Site	Altitude	Latitude[1]	Epoch	Effective latitude[2]	Primary data recalculated and scaled[3] atoms (g Ca)$^{-1}$ a^{-1}
Ca spallation						
Yokoyama et al. (1977)	Aiguille du Midi	3840 m	47°	Present day	47°	68 ± 14
Masarik and Reedy (1995)	High latitudes	Sea-level	> 60°	Present day	> 60°	64.6
This study	Tabernacle Hill	1445 m	38.9°	17.3 ka - present	40.9°	48.8 ± 1.7
Total production from Ca						
Zreda et al. (1991)	Tabernacle Hill	1445 m	38.9°	17.3 ka - present	40.9°	54.8 ± 5.0
Swanson et al. (1994)	Puget Sound	sea-level	47.4°	15.5 ka - present	48.2°	89.5 ± 5.6
This study	Tabernacle Hill	1445 m	38.9°	17.3 ka - present	40.9°	53.6 ± 1.8

(1) Latitude is geomagnetic for present-day calibrations, geographic for calibrations based on extended exposure.

(2) Calculated as discussed in Section 4.5 See Nishiizumi et al. (1989), Clark and Bierman (1995).

(3) Basis of all re-calculations discussed in Sections 4.5 and 4.6. Confidence limits are ± 1σ for results of this work; presumed ± 1σ where specified for other studies.

Table 5. Exposure ages for Sierra Nevada samples

Site / Sample	Thickness correction (2)	Horizon correction (3)	Carrier addition (4)	Weight (g)	[Ca] ($g\ g^{-1}$ in calcite)	[Cl] ($\mu g\ g^{-1}$ in calcite)	$\sigma_{35}N_{35}$ / $\Sigma\sigma_i N_i$ (5)	[^{36}Cl] (6) (10^6 atom g^{-1})	Exposure age cal. ka
Tioga Pass (37° 56' 15", 3005 m) (1)									
SGP-3(1)	0.965	0.988	-	17.027	0.400 ± 0.001	14.5 ± 1.1	0.00236 ± 0.00019	2.39 ± 0.13	14.7 ± 1.0
SGP-3(2)	0.965	0.988	-	7.578	0.400 ± 0.001	6.2 ± 0.5	0.00101 ± 0.00008	2.42 ± 0.14	15.0 ± 1.1
SGP-3(2)	0.965	0.988	+	6.794	0.400 ± 0.001	6.2 ± 0.5	0.00101 ± 0.00008	2.58 ± 0.15	15.9 ± 1.1
SGP-4(1)	0.961	0.966	-	16.384	0.391 ± 0.001	38.7 ± 1.9	0.00532 ± 0.00027	2.44 ± 0.08	14.9 ± 0.7
SGP-4(2)	0.961	0.966	-	5.922	0.391 ± 0.001	13.2 ± 0.5	0.00177 ± 0.00008	2.19 ± 0.13	14.3 ± 1.0
SGP-4(2)	0.961	0.966	+	4.861	0.391 ± 0.001	13.2 ± 0.5	0.00177 ± 0.00008	2.40 ± 0.15	15.3 ± 1.1
SGP-5	0.965	0.966	-	4.390	0.389 ± 0.001	30.4 ± 1.6	0.00373 ± 0.00021	2.35 ± 0.13	14.9 ± 1.0
SGP-5	0.965	0.966	+	6.132	0.388 ± 0.001	30.4 ± 1.6	0.00373 ± 0.00021	2.28 ± 0.14	14.5 ± 1.0
Gull Lake (37° 46' 22", 2356 m) (1)									
SGP-8	0.984	0.924	+	8.096	0.400 ± 0.001	30.5 ± 2.0	0.00439 ± 0.00030	2.55 ± 0.10	22.6 ± 1.2
SGP-10	0.976	0.941	-	16.122	0.400 ± 0.001	23.5 ± 1.1	0.00311 ± 0.00015	2.95 ± 0.26	26.5 ± 2.6

(1) Site details: Effective latitude for Tioga Pass over 14.9 cal. ka: 38.1°. Scaling factor for spallation and spallogenic neutrons: 8.37. Scaling factor for muon reactions: 3.32. Effective latitude for Gull Lake over 25 cal. ka: 42.3°. Scaling factor for spallation and spallogenic neutrons: 6.07. Scaling factor for muon reactions: 2.70.

(2) Correction relative to surface rate for spallation. Assumes exponential decrease from surface with attenuation length of 160g cm^{-2}. Production by muon capture and thermal neutron capture assumed constant over sample thicknesses (3 - 13 g cm^{-2}).

(3) Correction relative to 2Π irradiation geometry, assuming $Sin^{2.3}(\theta)$ zenith angle distribution for incoming flux as used by Nishiizumi et al. (1989). Other estimates for the value of the cosine exponent n for the fast neutron flux are $n = 2.1 \pm 0.3$ for 60 MeV neutrons and $n = 2.6 \pm 0.2$ (750 MeV neutrons); Conversi and Rothwell (1954); $n = 2.5 \pm 0.5$ (~ 200 MeV neutrons); Barford and Davis (1952); $n \sim 3$ (~ 100 MeV neutrons) and $n \sim 5$ (~ 1 GeV neutrons); Miyake et al. (1957) and $n = 3.5 \pm 1.2$ (integral spectrum 80 - 300 MeV neutrons); Heidbreder et al. (1971). Assuming a higher cosine exponent (more strongly collimated flux) would imply less shielding by surrounding obstructions, increased production and lower ages by 1 - 2% at Tioga Pass and ~ 3% at Gull Lake.

(4) "-" indicates carrier added before sample dissolution, "+" indicates carrier added after dissolution.

(5) Calculated from effective neutron absorption cross sections. Uncertainties based on analytical errors only (i.e. uncertainties in cross sections not propagated).

(6) Cosmogenic ^{36}Cl concentration, after subtraction of U-fission and (α,n)-produced ^{36}Cl. Corrections are < 0.1%. Uncertainties ± 1σ, including blank corrections, [Cl] and AMS errors.

between the results, when compared on a common basis, provides an encouraging interlaboratory comparison, however.

In a recent abstract, Swanson et al. (1994) have reported a value of 90 ± 6 atoms $(g\ Ca)^{-1}\ a^{-1}$ for the production rate of ^{36}Cl from calcium reactions at Puget Sound. The latitude of this site (47.4°N) makes production insensitive to geomagnetic effects over the 15.5 cal. ka exposure period. Assuming it applies to production at sea level, the rate determined by Swanson et al. (1994) is approximately 70% higher than the scaled values in Table 3.2. Without details of the underlying measurements and calculations, it is difficult to account for the discrepancy. It is possible that the factor used to scale the

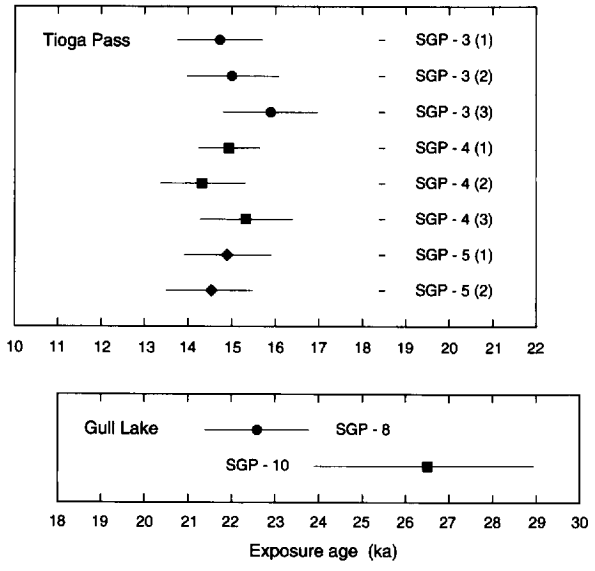

FIG. 3. Exposure age estimates for Sierra Nevada samples. Uncertainties (±1σ) based on full analytical errors and production rate uncertainties. Note age offset between Tioga Pass and Gull Lake sites.

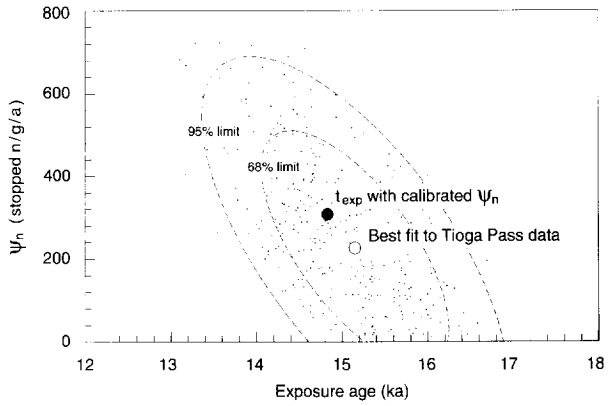

FIG. 4. Best fit (open symbol) and uncertainty limits on combined calculation of Tioga Pass exposure age and neutron capture rate ψ_n. Values of ψ_n scaled to sea-level and latitude > 60° for comparison with calibrated rate of 307 ± 24n $g^{-1}\ a^{-1}$ of Zreda et al. (1991), which gives 14.9 ka age for Tioga Pass surfaces (grey symbol). Confidence regions at 68 and 95% levels derived from the Monte-Carlo error distribution shown (small points). Note insensitivity of exposure age estimate to value of ψ_n.

Tabernacle Hill rate to sea level and high latitude is in error, but unlikely that this accounts for more than a small part of the difference.

A recent radiation transport calculation by Masarik and Reedy (1995) gives a calcium spallation rate at sea level and high latitude of 64.6 atoms (g Ca)$^{-1}$ a^{-1}, ~30% higher than the scaled value in Table 3.1. This discrepancy may also reflect, in part, the scaling procedure used to make the comparison. Note, however, that the nuclear modelling predicts ^{26}Al and ^{10}Be production rates similar to those derived from glacial pavements in the Sierra Nevada by Nishiizumi et al. (1989), who assumed a deglaciation age of 11 cal. ka. It is interesting, therefore, that if deglaciation of the pavements occurred earlier, as suggested by newly compiled ^{14}C ages for the range (Clark and Bierman, 1995; see also section 5 below), the empirical ^{26}Al and ^{10}Be production rates would also fall below the values predicted by the radiation transport calculation.

In summary, the previous whole-rock data from Tabernacle Hill (Zreda et al., 1991), when recalculated on the basis used in this work, yield a similar ^{36}Cl production rate from calcium. The scaled results of this study are lower than a number of estimated rates at sea level and high latitude, however. For the reasons discussed in section 4.3, the discrepancy is unlikely to be due to past shielding of the Tabernacle Hill flow. Alternatively, the factor used to scale production to sea level and high latitudes may be too high. A firm conclusion must await further calibration studies covering broader ranges of altitude, latitude, and exposure time.

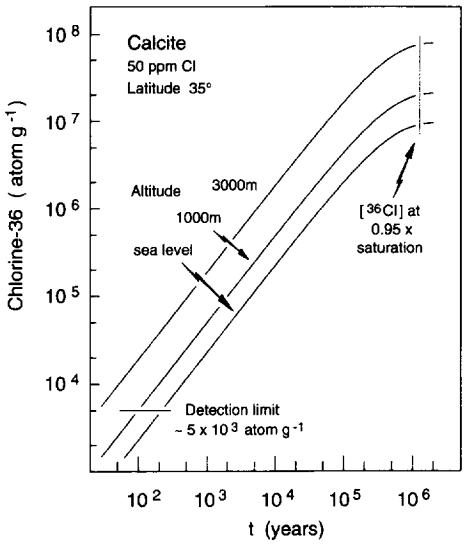

FIG. 5. Chlorine-36 accumulation in calcite at latitude 35° at sea level, 1000 and 3000 m altitude, compared to the detection limit discussed in section 3.4. The accumulation rates assume 50 ppm Cl, giving $(\sigma_{35}N_{35}/\Sigma\sigma_i N_i) \sim 0.01$, hence ~13% of total production due to neutron capture at sea level. Cosmogenic ^{36}Cl should be detectable after as little as 30 years exposure at high altitudes. The time at which concentrations become indistinguishable from saturation values (90–95% of saturation) is an upper limit for exposure dating. On most terrestrial surfaces, erosion can be expected to reduce this limit significantly.

4.7. Comparison with Nuclear and Cosmic Ray Data

The results of this work can also be combined with measured spallation rates (star production rates) to derive the ^{36}Cl yield from calcium at cosmic ray energies. The calculation proceeds from the total disintegration rate in air at sea level and high latitude, taken as ~560 g^{-1} a^{-1} (Lal and Peters, 1967). For convenience, this is converted to a calcium disintegration rate in calcite in order to determine the ^{36}Cl yield. Assuming geometric cross sections, the total spallation rate in calcite would be ~490 g^{-1} a^{-1}, and the proportion of calcium stars 33%. The ^{36}Cl production rate of 19.5 atoms g^{-1} a^{-1} in calcite is then equivalent to 12% of spallations on calcium. This yield for $(3p2n)$ emission is higher than the estimated yields of ^{36}Cl and ^{35}S from similar $(p3n)$ and $(2p3n)$ reactions on ^{40}Ar; 7.7% and 9.5%, respectively (Lal and Peters, 1967), but is not unreasonable for the expected peak in spallation yield at 4–5 nucleon emission.

5. COSMOGENIC CHLORINE-36 IN CALCITE

Because of its exceptionally high calcium content, calcite is a favourable target mineral for ^{36}Cl production. The spallation and muon capture rates in Table 3.1 indicate a ^{36}Cl production rate of 21.4 atoms g^{-1} a^{-1} in calcite at sea level and high latitude, which would be further supplemented by thermal neutron-capture production. At the low chlorine concentrations we have encountered in most calcite samples, neutron capture makes a minor contribution, however. Most calcite exposure ages are therefore insensitive to the complexities of near-surface neutron production and thermalisation (O'Brien et al., 1978; Dep et al., 1994). The experiment described in section 3.2 confirms that calcite retains ^{36}Cl produced in situ.

To investigate exposure dating of calcite, we measured five samples from glacially abraded limestone outcrops at Gull Lake and Tioga Pass in the Sierra Nevada. The aim of the measurements is to date exposure of these outcrops by ice retreat at the end of the Tioga glacial stage (Blackwelder, 1931; Clark and Bierman, 1995). Geographic details of the sites and the factors used to scale production rates are listed in Table 5. Latitude scaling factors were calculated iteratively, refining estimates of age and effective latitude in turn (see section 4.5).

At Tioga Pass, samples of metamorphosed limestone were collected from thin beds in quartzite near Ellery Lake. At Gull Lake marble was collected from bands in the face of a prominent quartzite *roche moutonée*. In both cases, limestone was found to have eroded 1–1.5 cm below the level of glacial polish on the adjacent quartzite surfaces. Erosion rates of ~1 × 10^{-4} cm a^{-1} have therefore been incorporated into the age calculations. Neglecting erosion would result in ages underestimated by 1–2%. In both cases, samples were taken from open, south-facing outcrops with dips between 10 and 25° to promote melting of winter snow and minimise its winter shielding effects.

Exposure ages for the samples are given in Table 5 and shown in Fig. 3. These can be compared to a recent compilation of ^{14}C ages for postglacial deposits in the Sierra Nevada (Clark and Bierman, 1995) which indicates that Tioga Stage

retreat was underway, at least on the lower western face of the range, by 18–16 cal. ka BP. Ages of postglacial sediment at higher elevations and on the eastern side of the range are generally younger, mostly in the interval 15–13 cal. ka BP. Both sites sampled in this work lie outside the limits of the minor Recess Peak re-advance and are therefore expected to have deglaciation ages older than the termination of that stage around 13.1 cal. ka (Clark and Bierman, 1995). In comparing exposure ages with this chronology, it should be remembered that deglaciation must predate sedimentary deposits at a site and that local climatic factors may have delayed or promoted glacial retreat in different ice drainages.

Although the Gull Lake samples were collected only a few kilometres behind the outermost Tioga Stage moraines and would therefore be expected to record an early phase of retreat, their apparent ages are implausibly high. Since their ages are also barely consistent with one another, this may be due to shallow and variable erosion during the Tioga advance, failing to remove preexisting cosmogenic ^{36}Cl. If so, the younger "age" is merely an upper limit to the age of deglaciation. Interestingly, these results mimic anomalously high ^{26}Al and ^{10}Be concentrations in quartz from nearby outcrops at June Lake, which were also attributed to inadequate subglacial erosion (Nishiizumi et al., 1989).

Samples from Tioga Pass, though collected from separate outcrops likely to have experienced different amounts of subglacial erosion, give concordant exposure ages (Table 5). This implies removal of pre-existing cosmogenic ^{36}Cl by thorough subglacial scouring. The proximity of the site to a major break in slope of the glacier bed (below what is now Ellery Lake) may have assisted erosion by increasing local ice velocity (Drewry, 1986). The average age given by the three surfaces is 14.9 cal. ka, with a standard deviation from the eight measurements of ±0.5 ka. No allowance has been made for shielding by winter snow; hence, the result may slightly underestimate the true deglaciation age. The likely magnitude of this effect can be gauged from precipitation at Ellery Lake, adjacent to the sample site. Over the past sixty-two years, the site has received an average of 47 g cm^{-2} of winter precipitation (NCDC, 1995). Under the most conservative assumptions, that this amount falls entirely as snow and is retained for six months, the spallation rate at the rock surface would be decreased by approximately 14%. The actual effect on the exposure ages is likely to be smaller, since these assumptions are pessimistic and the outcrops sampled were chosen to minimise retention of snow. In addition, pollen records from lake cores suggest more arid conditions in the region for much of the exposure period (Anderson and Smith, 1994). The ages accord with the generalised deglaciation history of Clark and Bierman (1995), indicating that the site was free of ice prior to the ~13.1 ka Recess Peak re-advance, which produced small cirque glaciers approximately 400 m higher in elevation and several kilometres up-valley in the Tioga Pass area.

Presuming that the samples share a common exposure history, it is possible to use the variations in their ^{36}Cl concentration and Cl/Ca ratio to obtain an estimate of the neutron capture rate ψ_n. A similar χ^2 fitting procedure to that of section 4.4 gives the values of exposure age and neutron stopping rate ψ_n which maximise agreement between calculated and measured ^{36}Cl concentrations. As shown in Fig. 4, the result of the calculation scaled to sealevel and high latitude (section 4.5) is a neutron stopping rate of $220^{+490}_{-220}n$ g^{-1} a^{-1}, which is at least consistent with the calibrated value of 307 ± 24n g^{-1} a^{-1} (Zreda et al., 1991). The poor constraint afforded by the samples is due to Cl/Ca ratios $< 10^{-4}$, as a result of which production by neutron capture accounts for only 1–5% of their total ^{36}Cl. Since this is less than the typical uncertainty of the ^{36}Cl measurements, the calculation fails to improve on the existing value of ψ_n. Nonetheless, the best estimate of exposure age obtained without constraint on ψ_n is indistinguishable from the age obtained with ψ_n fixed. The error bounds shown in Fig. 4 highlight the insensitivity of calcite exposure ages to precise knowledge of the neutron-capture rate.

6. CONCLUSIONS AND PROSPECTS

We have measured ^{36}Cl in Ca-rich target minerals and calibrated its near-surface production rate. This will allow precise exposure dating, at least at mid-latitudes and similar elevation to the calibration site. Further calibration of the production rate may be required to address discrepancies with estimates for high latitudes, however.

Among potential target minerals, calcite has the highest calcium concentration and therefore the greatest ^{36}Cl accumulation rate. As shown in Fig. 5, the production rates determined above combined with the detection limit discussed in section 3.4 lead to measurable abundances of ^{36}Cl in calcite after 300 years exposure at sea level, and as little as 30 years exposure at sites such as Tioga Pass. Modifications to the routine procedures described in section 2 (such as increasing sample sizes, decreasing the amount of carrier used, and extending counting times) could improve these limits further. The target chemistry of calcite simplifies exposure measurements in a number of ways. The absence of potassium reduces the number of ^{36}Cl-producing reactions which need to be taken into account. The low chlorine concentrations of many calcite samples (and the high macroscopic cross sections of most limestones) suppress ^{36}Cl production by neutron capture, with its complicated depth and compositional dependences. Also, because production from calcium greatly outweighs production from chlorine, errors in chlorine measurements contribute less to final errors in exposure ages measured on calcite than on minerals and rocks in which chlorine is a major target element.

Interestingly, the compositions of calcite and Ca-bearing silicates also favour production of cosmogenic ^{10}Be and ^{41}Ca. Though the combined abundance of oxygen and carbon in calcite is slightly less than the abundance of oxygen in quartz, the yield of the ^{12}C(n, $2pn$)^{10}Be reaction (Q = −27.2 MeV) can be expected to be higher than the equivalent reaction on ^{16}O (Q = −54.6 MeV). A ^{10}Be production rate of 5–10 atoms g^{-1} a^{-1}, similar to that in quartz, can be anticipated. The possibility of measuring ^{41}Ca in calcite has already been explored (Fink et al., 1990). Production is from neutron capture on ^{40}Ca alone (σ = 0.41b), unfortunately resulting in fairly low ^{41}Ca/^{40}Ca ratios, on the order of 10^{-14} at sea level and 10^{-13} at high altitudes. Calcium-41 measurements could either be used independently for exposure dating (requiring

knowledge of the neutron stopping rate ψ_n) or to eliminate the neutron stopping rate from age measurements based on ^{36}Cl (since ^{36}Cl produced by neutron capture could be calculated from the ^{41}Ca concentration and the ratio of cross sections, and subtracted from the total ^{36}Cl in the sample). Combining measurements of these three isotopes, with half-lives of 1.5×10^6, 3×10^5, and 1×10^5 years would open up a range of possibilities for deciphering complex exposure histories.

Acknowledgments—We gratefully acknowledge assistance with fieldwork from Mark Fahnestock in the Sierra Nevada and Thure Cerling at Tabernacle Hill. Elmer Kiss, Mike Shelley, and Audrey Chapman assisted with the chemistry at various stages. Les Kinsley, Paul Sylvester, Steve Eggins, and Malcolm McCulloch facilitated trace element measurements by ICP–MS. Marek Zreda generously provided suggestions on extraction chemistry at an early stage of the work. Extensive discussions with Paul Bierman, Alan Gillespie, and Doug Clark, and thoughtful reviews by Bob Reedy and Terry Swanson contributed to the manuscript at various stages.

Editorial handling: F. M. Phillips

REFERENCES

Anderson R. S. and Smith S. J. (1994) Palaeoclimatic interpretations of meadow sediment and pollen stratigraphies from California. *Geology* **22,** 723–726.

Bard E., Hamelin B., Fairbanks R. G., and Zindler A. (1990) Calibration of the ^{14}C timescale over the past 30,000 years using mass spectrometric U-Th ages from Barbados corals. *Nature* **345,** 405–410.

Bard E., Arnold M., Fairbanks R. G., and Hamelin B. (1993) ^{230}Th-^{234}U and ^{14}C ages obtained by mass spectrometry on corals. *Radiocarbon* **35,** 191–199.

Barford N. C. and Davis G. (1952) The angular distribution and attenuation of the star-producing component of cosmic rays. *Proc. Roy. Soc. London* **A 214,** 225–237.

Bentley H. W., Phillips F. M., and Davis S. N. (1986) Chlorine-36 in the terrestrial environment. In *Handbook of Environmental Isotope Geochemistry* (ed. P. Fritz and J. C. Fontes), pp. 427–480. Elsevier.

Blackwelder E. (1931) Pleistocene glaciation in the Sierra Nevada and Basin Ranges. *Bull. GSA* **42,** 865–922.

Cerling T. E. (1990) Dating geomorphologic surfaces using cosmogenic ^{3}He. *Quat. Res.* **33,** 148–156.

Clark D. H. and Bierman P. R. (1995) Accurate ^{10}Be and ^{26}Al chronologies require improved production-rate calibration. *Quat. Res.* (in press).

Conard N. J., Elmore D., Kubik P. W., Gove H. E., Tubbs L. E., Chrunyk B. A., and Wahlen M. (1986) The chemical preparation of AgCl for measuring ^{36}Cl in polar ice with accelerator mass spectrometry. *Radiocarbon* **28,** 556–560.

Conversi M. (1950) Experiments on cosmic-ray mesons and protons at several altitudes and latitudes. *Phys. Rev.* **79,** 749–767.

Conversi M. and Rothwell P. (1954) Angular distribution in cosmic ray stars at 3500 meters. *Nuovo Cimento* **12,** 191–209.

Craig H. and Poreda R. J. (1986) Cosmogenic ^{3}He in terrestrial rocks: the summit lavas of Maui. *Proc. Natl. Acad. Sci. U.S.A.* **83,** 1970–1974.

Davis R. J. and Schaeffer O. A. (1955) Chlorine-36 in nature. *Ann. N.Y. Acad. Sci.* **62,** 105–122.

Dep L., Elmore D., Fabryka-Martin J., Masarik J., and Reedy R. C. (1994) Production rate systematics of in situ produced cosmogenic nuclides in terrestrial rocks: Monte Carlo approach of investigating ^{35}Cl(n, γ)^{36}Cl. *Nucl. Instr. Meth.* **B92,** 321–325.

Drewry D. (1986) *Glacial Geologic Processes.* Edward Arnold.

Evans K. L., Tarter J. G., and Moore C. B. (1981) Pyrohydrolytic-ion chromatographic determination of fluorine, chlorine and sulfur in geological samples. *Anal. Chem.* **53,** 925–928.

Fabryka-Martin J. T. (1988) Production of radionuclides in the earth and their hydrogeologic significance, with emphasis on chlorine-36 and iodine-129. Ph.D. dissertation, Univ. Arizona.

Fifield L. K., Ophel T. R., Allan G. L., Bird J. R., and Davie R. F. (1990) Accelerator mass spectrometry at the Australian National University's 14UD accelerator: experience and developments. *Nucl. Instr. Methods Phys. Res.* **B52,** 233–237.

Fifield L. K., Allan G. L., Stone J., and Ophel T. R. (1994) The ANU AMS system and research program. *Nucl. Instr. Meth.* **B92,** 85–89.

Fink D., Klein J., and Middleton R. (1990) ^{41}Ca: Past, present and future. *Nucl. Instr. Meth.* **B52,** 572–582.

Florence T. M. and Farrar Y. J. (1971) Spectrophotometric determination of chloride at the parts-per-billion level by the mercury(II) thiocyanate method. *Anal. Chim. Acta* **54,** 373–377.

Heidbreder E., Pinkau K., Reppin C., and Schönfelder V. (1971) Measurements of the distribution in energy and angle of high-energy neutrons in the lower atmosphere. *J. Geophys. Res.* **76,** 2905–2916.

Klein J., Middleton R., Giegengack R., and Sharma P. (1988) Revealing histories of exposures using in situ produced ^{26}Al and ^{10}Be in Libyan desert glass. *Radiocarbon* **28,** 547–555.

Klein J., Macchiaroli P., Giegengack R., Middleton R., Lawn B., and Dezfouly-Arjomandy B. (1993) Late Cenozoic history of East Antarctica, inferred from measurement of cosmogenic ^{10}Be and ^{26}Al, produced in-situ on exposed bedrock surfaces. *Eos Trans. Amer. Geophys. Union* **74,** 154 (abstr.).

Kubik P. W., Korschinek G., Nolte E., Ratzinger U., Ernst H., Teichmann S., Morinaga H., Wild E., and Hille P. (1984) Accelerator mass spectrometry of ^{36}Cl in limestone and some paleontological samples using completely stripped ions. *Nucl. Instr. Meth.* **B5,** 326–330.

Kurz M. D. (1986) Cosmogenic helium in a terrestrial igneous rock. *Nature* **320,** 435–439.

Lal D. (1988) In situ produced cosmogenic isotopes in terrestrial rocks. *Annu. Rev. Earth Planet. Sci.* **16,** 355–388.

Lal D. (1991) Cosmic ray labeling of erosion surfaces: in situ nuclide production rates and erosion models. *Earth Planet. Sci. Lett.* **104,** 424–439.

Lal D. and Peters B. (1967) Cosmic ray produced radioactivity on the earth. In *Handbuch der Physik* (ed. S. Flugg), Vol. XLVI/2, pp. 551–612. Springer.

Lingenfelter R. E., Canfield E. H., and Hampel V. E. (1972) The lunar neutron flux revisited. *Earth Planet. Sci. Lett.* **16,** 355–369.

Masarik J. and Reedy R. C. (1995) Terrestrial cosmogenic-nuclide production systematics calculated from numerical simulations. *Earth Planet. Sci. Lett.* (in press).

McElhinny M. W. and Senanayake W. E. (1982) Variations in the geomagnetic dipole 1: The past 50,000 years. *J. Geomag. Geoelectr.* **34,** 39–51.

Meynadier L., Valet J.-P., Weeks R., Shackleton N. J., and Hagee V. L. (1992) Relative geomagnetic intensity of the field during the last 140 ka. *Earth Planet. Sci. Lett.* **114,** 39–57.

Miyake S., Hinotani K., Katsumata J., and Kaneko T. (1957) Cosmic ray nuclear interaction in nitrogen gas. *J. Phys. Soc. Japan* **12,** 845–854.

NCDC (1995) California co-operative precipitation records. U.S. National Climatic Data Center, National Oceans and Atmosphere Administration.

Nishiizumi K., Winterer E. L., Kohl C. P., Klein J., Middleton R., Lal D., and Arnold J. R. (1989) Cosmic ray production rates of ^{10}Be and ^{26}Al in quartz from glacially polished rocks. *J. Geophys. Res.* **94,** 17,907–17,915.

Nishiizumi K., Kohl C. P., Arnold J. R., Klein J., Fink D., and Middleton R. (1991a) Cosmic ray produced ^{10}Be and ^{26}Al in Antarctic rocks: exposure and erosion history. *Earth. Planet. Sci. Lett.* **104,** 440–454.

Nishiizumi K., Kohl C. P., Shoemaker E. M., Arnold J. R., Klein J., Fink D., and Middleton R. (1991b) In-situ ^{10}Be-^{26}Al exposure ages

at Meteor Crater, Arizona. *Geochim. Cosmochim. Acta* **55,** 2699–2703.

Nishiizumi K., Kohl C. P., Arnold J. R., Dorn R., Klein J., Fink D., Middleton R., and Lal D. (1993) Role of in situ cosmogenic nuclides ^{10}Be and ^{26}Al in the study of diverse geomorphic processes. *Earth Surf. Proc. Landforms* **18,** 407–425.

O'Brien K., Sandmeier H. A., Hansen G. E., and Campbell J. E. (1978) Cosmic ray induced neutron background sources and fluxes for geometries of air over water, ground, iron and aluminium. *J. Geophys. Res.* **83,** 114–120.

Oviatt C. G. and Nash W. P. (1989) Late Pleistocene basaltic ash and volcanic eruptions in the Bonneville basin, Utah. *GSA Bull.* **101,** 292–303.

Phillips F. M., Leavy B. D., Jannik N. D., Elmore D., and Kubik P. W. (1986) The accumulation of cosmogenic chlorine-36 in rock; a method for surface exposure dating. *Science* **231,** 41–43.

Phillips F. M., Zreda M. G., Smith S. S., Elmore D., Kubik P. W., and Sharma P. (1990) A cosmogenic chlorine-36 chronology for glacial deposits at Bloody Canyon, Eastern Sierra Nevada, California. *Science* **248,** 1529–1532.

Phillips F. M., Zreda M. G., Smith S. S., Elmore D., Kubik P. W., Dorn R. I., and Roddy D. J. (1991) Age and geomorphic history of Meteor Crater, Arizona, from cosmogenic ^{36}Cl and ^{14}C in rock varnish. *Geochim. Cosmochim. Acta* **55,** 2695–2698.

Poreda R. J. and Cerling T. E. (1992) Cosmogenic neon in recent lavas from the western United States. *Geophys. Res. Lett.* **19,** 1863–1866.

Stone J., Allan G. L., Fifield L. K., Evans J. M., Cresswell R. G., and Chivas A. R. (1994) Limestone erosion measurements with cosmogenic chlorine-36 in calcite—preliminary results from Australia. *Nucl. Instr. Meth.* **B 92,** 311–316.

Stone J., Lambeck K., Fifield L. K., Cresswell R. G., and Evans J. M. (1995) Cosmogenic isotope constraints on shoreline erosion and sea-level change—a Lateglacial age for the Main Rock Platform, Western Scotland. *Geology* (submitted).

Stuiver M. and Reimer P. J. (1993) Extended ^{14}C data base and revised CALIB 3.0 ^{14}C age calibration program. *Radiocarbon* **35,** 215–230.

Swanson T. W., Caffee M. W., Finkel R. C., Harris L., and Southon J. (1994) Application of 36Cl dating based on the deglaciation history of the Cordilleran ice sheet in Washington and British Columbia. *GSA 1994 Annual Meeting, Abstr. with Prog. A-512* (abstr.).

Winsberg L. (1956) The production of chlorine-39 in the lower atmosphere by cosmic radiation. *Geochim. Cosmochim. Acta* **9,** 183–189.

Yokoyama Y., Reyss J.-L., and Guichard F. (1977) Production of radionuclides by cosmic rays at mountain altitudes. *Earth Planet. Sci. Lett.* **36,** 44–50.

Zreda M. G. (1994) Development and calibration of the cosmogenic ^{36}Cl surface exposure dating method and its application to the chronology of late Quaternary glaciations. Ph.D. dissertation, New Mexico Institute of Mining and Technology Socorro.

Zreda M. G., Phillips F. M., Elmore D., Kubik P. W., and Sharma P. (1991) Cosmogenic chlorine-36 production rates in terrestrial rocks. *Earth Planet. Sci. Lett.* **105,** 94–109.